

<https://doi.org/10.1038/s40494-025-01735-6>

# Reassessment of the Penglai III shipwreck and reflections on the wooden artifacts conservation

Check for updates

Yishu Wang<sup>1,2</sup>, Li Liu<sup>3</sup>, Shuangcheng Wu<sup>4</sup>, Zhimin Li<sup>1,2</sup> & Qinglin Ma<sup>5</sup>✉

The conservation of marine archaeological wooden shipwrecks remains a global challenge. The Penglai III shipwreck provides a good case study to examine the state and condition of a wooden shipwreck after nearly 20 years of conservation treatments, especially to assess the effects of PEG hardening treatments and mineral in the wood. Analytical techniques, including ultra-deep far-field 3D microscopy, environmental scanning electron microscopy (ESEM-EDS), micro-Raman spectrometry (Raman), and Fourier transform infrared spectroscopy (FT-IR), were employed. Results indicated that PEG initially aided in drying and strengthening the wood, but prolonged air exposure caused darkening, affecting its visual appearance. This triggered the assessment of the drying and strengthening treatment of wooden shipwrecks and the selection of materials. Wood was rich in iron deposits and calcium deposits, which may lead to acidification and further degradation over time. Environmental control is recommended as a priority for future conservation efforts. This study provides valuable insights into the conservation and restoration of marine wooden shipwrecks.

Penglai Water City(蓬莱水城), also known as Dengzhou(登州) Port, has served as a crucial nexus for foreign trade in northern China since antiquity (Fig. 1), playing a pivotal role in connecting the Oriental Maritime Silk Road. In both 1984 and 2005, archaeological expeditions conducted extensive dredging operations in the central maritime zone of Penglai Water City, resulting in the discovery of four shipwrecks. Among them, the Penglai III shipwreck was excavated in 2005. Subsequent investigations identified it as a relic from the Korean Goryeo(高丽) period, dating back to the transition between the late Yuan(元代) and early Ming Dynasty(明代) 1368 ~ 1444 AD). Notably, the overall preservation of the hull is remarkably intact, bearing significant implications for the study of Dengzhou's role and status along China's ancient Maritime Silk Road<sup>1</sup>.

Marine wooden shipwrecks are very fragile organic cultural relics that are highly susceptible to degradation and decay due to environmental changes. Penglai III shipwreck was unearthed in July 2005<sup>2</sup>; the summer sun's exposure inevitably caused the water saturation of the ship's wood to rapid dehydration, resulting in the ship's wood cracking, warping, layer, and other phenomena. To avoid the hull wood being affected by environmental factors, archaeologists built a sunshade over the excavation site, effectively preventing the sun's exposure to the hull. The awning of the semi-closed

enclosure's south, west, and north sides relieves water evaporation, creating a relatively suitable environment for excavation and protection. Penglai III shipwreck was covered with silt and sprayed with water to keep them moist due to the severe corrosion and *Nereis Succinea* erosion of their hulls and the depth of the buried layer. Specific practice is to cover the hull's surface with a layer of silt, which is covered with straw, towards the straw on the water spray to create a moisturizing effect<sup>3</sup>.

At the excavation site, when the surface of the ship's hull had been exposed (Fig. 2), the lower part was still buried in the silt. The conservators took the measure of spraying medical alcohol on the surface of the ship's timber to inhibit the growth of bacteria on the surface of the ship's wood. Then, they started to spray 5% ~ 10% PEG2000 to strengthen the hull. After that, they sprayed a mixture of 12.5% PEG4000 and 0.4% borax to dehydrate the wreck and reinforced wood. This prevented rapid evaporation of water from the wood and prevented microbial growth on the hull surface. The wreck was dismantled before the winter of 2005, and the timbers were moved indoors (museum) to continue conservation work<sup>3</sup>.

At that time, after the timbers were transferred indoors, it was racked and placed off the ground to facilitate the spillage of water molecules in the waterlogged wood and the penetration of protective materials such as

<sup>1</sup>Joint International Research Laboratory of Environmental and Social Archaeology, Shandong University, Qingdao, 266237 Shandong Province, China. <sup>2</sup>Institute of Cultural Heritage, Shandong University, Qingdao, Shandong, 266237, China. <sup>3</sup>Penglai Ancient Ship Museum, Yantai, 265699 Shandong Province, China.

<sup>4</sup>Shandong Provincial Cultural Relics Conservation, Restoration and Identification Center, Jinan, 250014, China. <sup>5</sup>Key Scientific Research Base of Science & Technology Evaluation, National Cultural Heritage Administration (Beijing University of Chemical Technology), Beijing, 100029, China.

✉e-mail: [Qinglinma226@126.com](mailto:Qinglinma226@126.com)

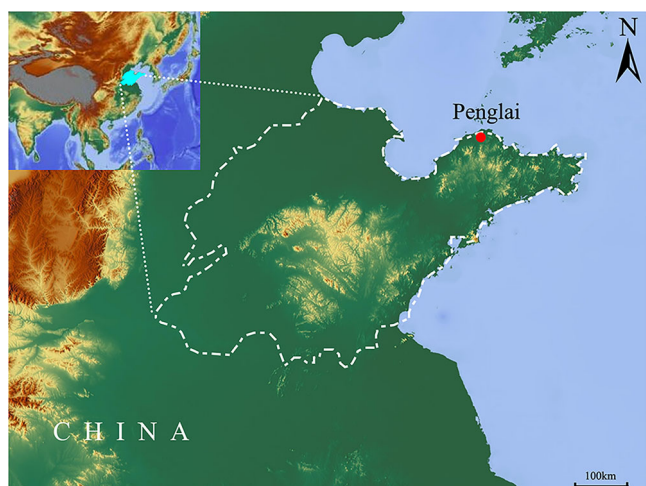


**Fig. 1** | Geographical location map of Penglai Water City (The red dots indicate the location of Penglai).



**Fig. 2** | A photo of the Penglai III shipwreck after it has been archaeologically excavated and cleaned up.

polyethylene glycol, which also effectively avoided the phenomenon of rotting of the ship's timbers. They cleaned the pollutants such as mud and sand attached to the hull's surface of the hull, so that all the wood color of the ship's timber was revealed, and also facilitated the penetration of the spray chemical protection material. In the indoor protection phase, the chemical sprayed was a mixture of PEG with a molecular weight of 4000 at a concentration of 12.5%, borax at 0.4%, and Peregal (natural fatty alcohol adducts with ethylene oxide) at 0.3%, sprayed once a day in the morning and once a day in the evening. Through the spraying of chemical protection reagents and many tests, the conservator found that the PEG-based chemical protection reagent for many low-temperature spraying is prone to white film phenomenon, resulting in poor penetration of the PEG. Therefore, the constructor physically removes the white film from the surface of the wood (using tools such as scalpels, bamboo sticks, etc.) at regular intervals during the construction process to ensure that the chemical protection reagents penetrate as fully as possible. Since the summer of 2008, the application number of times the chemical protection reagent spraying has increased, taking advantage of the high summer temperatures and the easier penetration of the chemical protection reagent sprayed on the ship materials of the ancient ships to change the frequency of spraying to three times in the morning, midday and evening to spray the chemical protection reagent. To speed up the speed of chemical protection reagent penetration of the shipping material, to promote shipwreck protection. The desalination of shipwrecks is mainly to utilize the water in the daily spraying of chemical protection reagents to continuously remove the salt of the ancient ship materials, to achieve the purpose of gradual desalination. In the process of



**Fig. 3** | A photo about the Penglai III shipwreck on display in the museum.

dewatering and drying, wetted paper pulp has also been applied to the surface of the hull to remove the sedimentary salt precipitated on the surface of the ship's wood<sup>2,3</sup>.

Meanwhile, after the shipwreck was moved indoors, the temperature and humidity in the museum were bullied by seasonal changes. Therefore, building a shed indoors and temperature control equipment to maintain the environmental temperature where the shipwreck is located at 15 ~ 20 °C, with humidity at 65 ~ 70% RH. After 2010, the old ship entered into the late-stage protection project; in December 2010, it stopped spraying the original chemical protection materials and replaced them with new protection materials for the late-stage protection of the old ship. The new material is 1% lignin, 2% calcium xanthate (sprayed for 3 months), and 4% calcium xanthate solution sprayed once a day to increase the lignin in the ancient ship's timber to increase the strength of the ship's timber.

In March 2012, the ship materials of the Penglai III shipwreck were transported into the newly completed Penglai Ancient Ship Museum and restored and assembled at the original site of the discovery of the ancient ships (Fig. 3). According to the order of building up keel piers and side piers, placing the keel on the piers, connecting the left and right bottom boards and outer boards, and then adding bulkhead boards and ribs, the restoration project was finally completed.

Generally speaking, during the period from the excavation in 2005 to 2012, protective measures such as dehydration and drying, reinforcement, bacterial and mold inhibition, and environmental control were taken for the ancient shipwreck, which had achieved certain effects at that time and undoubtedly played a certain positive role in the preservation of the ancient shipwreck so far. However, the excavation of the ancient ship has been going on for 20 years, and now there are new challenges and problems. Now, the overall surface of the shipwreck has turned black, and the local precipitation of yellowish-brown and reddish-brown deposits may be harmful to preserving the shipwreck. To understand the reasons for the discoloration of the shipwreck, the composition of the deposits precipitated from the wood, and to analyze their possible impact on the preservation of the shipwreck in the future, this paper has carried out analytical and testing work in several aspects, such as the drying and consolidation of the wood, the degree of degradation of the wood, and the composition and distribution of deposits in the wood, and have studied the various properties of the wood of the ship's hull. This research is not only a further assessment of the previous shipwreck protection materials and methods but also simultaneously triggered reflection and thinking on the protection work, which laid the foundation for the subsequent protection and restoration of Penglai III shipwreck and also provided inspiration for the protection of marine wooden cultural relics.

## Methods

### Samples collection

The remains of this ancient vessel measure approximately 17.10 meters in length and 6.20 meters in width, with a cabin depth of 1.28 meters. The

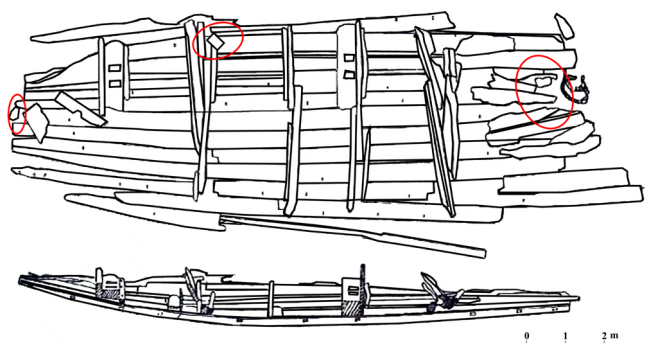


**Fig. 4** | Plan view line drawing of the Penglai III Shipwreck (red oval circles indicate the primary sampling areas).

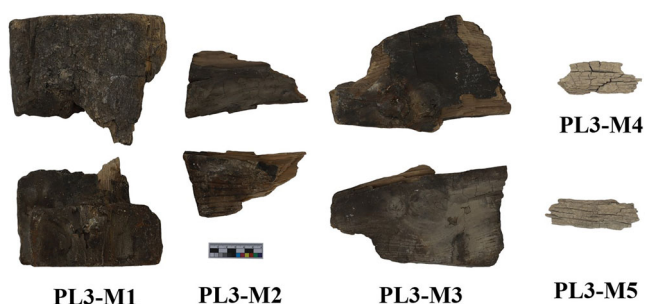


**Fig. 5** | Digital photograph of wood samples (PL3-M1~M5) of Penglai III shipwreck.

wreck of Penglai III was in a dry state, and three samples of wood ((PL3-M1, PL3-M2, and PL3-M3) were collected from the surface of the hull (Fig. 4). The thickness of PL3-M1 was about 7 cm, and the thickness of PL3-M2 and PL3-M3 was about 3 cm. The surfaces of the samples were all blackened and darkened, but the interior retained the wood's original color. In addition, white substances and reddish-brown and yellowish-brown rust stains were unevenly distributed on the surface of the samples. Two pieces of wood (PL3-M4 and PL3-M5) were also collected that had not undergone any conservation treatment since the excavation to compare the effect of previous conservation treatments. These two samples were around 3 cm thick and had multiple surface cracks in different directions (Fig. 5). These five samples were all pine (*Pinus* spp.), based on the tree species identification of the Penglai III shipwreck in 2005 and the labels of different parts of the ship's hull recorded by the museum<sup>1</sup>. The hull of the Penglai III shipwreck was made almost entirely of pine. This is mainly because this ship was used as a commercial cargo ship in ancient times, and was designed to increase its buoyancy by reducing its weight, thereby increasing its cargo-carrying capacity. Pine's low density, low specific gravity, and high buoyancy made it a suitable choice.

It is important to note that the Penglai III shipwreck is a unique cultural resource for the museum, and destructive sampling was limited. Despite the limited number of wood samples that could be collected, preserving the various parts of the ship's hull was relatively similar. Therefore, the samples collected represent not only these particular pieces of wood but, to a certain extent, also give us an idea of the overall condition of the wreck.

#### Fourier transform infrared spectroscopy (FT-IR)

The different properties of wood samples from the Penglai III shipwreck were analyzed and tested. To assess the aging degradation of wood, samples collected were analyzed using a Fourier Transform (Micro) Infrared (FTIR) spectrometer (Thermo Fisher Scientific). Considering that the residual PEG in the samples may affect the test results, a certain amount of uncontaminated wood flour is scraped from the surface of PL3-M1, M2, M3, M4, and M5. The wood flour is shaken and soaked in deionized water at 50°C for

8 hours, changing the deionized water every 2 hours. The samples were then soaked in anhydrous ethanol for two weeks, changing the ethanol solution every two to three days. Thus, after removing as much PEG as possible from the sample, the sample was dried and analyzed by infrared spectroscopy. The operation was repeated and measured three times for each sample. The instrument is equipped with a micro-infrared mainframe (Nicolet iN10), an attenuated total reflection (ATR) accessory, and a transmission accessory (Nicolet iS10/iZ10 auxiliary optics platform). Measures the surface of treated wood samples at ambient temperature. Thirty-two scans in the 400–4000  $\text{cm}^{-1}$  range were performed, and the average spectra were collected with a spectral resolution of 4  $\text{cm}^{-1}$ . The spectra were analyzed using OMNIC™ software.

#### Environmental water content (EMC) analysis

The current drying of the wood was assessed by calculating the equilibrium moisture content of different samples. The average temperature inside the Penglai Ancient Boat Museum at the time of sample collection was approximately 20 °C, and the humidity was 65% RH. The samples were kept in plastic bags when retrieved from the museum, and immediately after the retrieval, some of them were cut into small pieces of wood of 1 cm × 1 cm × 1 cm and weighed as  $M_{RH}$ . Small fragments of sound pine wood were placed in an environmental chamber with a constant temperature and humidity (20 °C, 65% RH) for 5 days and weighed its mass. These samples were then oven-dried to constant weight, and their dried mass was weighed and recorded as  $M_0$ . These samples' equilibrium moisture content was calculated using Eq. (1).

$$EMC = (M_{RH} - M_0) / M_0 \times 100\% \quad (1)$$

#### pH analysis

According to “GB/T 6043-2009”, the acidification of wood is determined<sup>4</sup>. Four different parts of each wood sample were taken, two parts that were seriously contaminated by rust and two cleaner parts, and the pH values of these four parts were determined, respectively. The testing equipment was a Seven Compact pH meter with an operating ambient temperature of 22 °C.

#### Ultra-deep far-field 3D microscopy

In addition, the Leica 3D Video Microscope DVM6P was used to observe the surface microscopic morphology of the loose wood samples, especially to observe the enrichment of deposits on the surface of the samples. The standard magnification of the microscope is 50X–1000X, and the camera is a 2/3-inch CCD chip with 1394 card acquisition, 5 million physical pixels, and 12-bit bit depth.

#### Environmental scanning electron microscopy (ESEM-EDS)

Microscopic morphology of the sample surface and interior was observed using an environmental scanning electron microscope (Thermo Scientific, Quattro S) with a Bruker QUANTAX EDS X-ray energy spectrometer. For example, the filling and consolidation of wood can be determined from the internal tubular cell structure and the shape of the cell wall voids. The crystal morphology of sediments can be visualized under the SEM to detect the elemental and content of the sediments to determine their composition. ESEM standard detectors include ETD, low vacuum LVD, gaseous SED (GSED) for ESEM mode, and IR camera. Low vacuum and ESEM capabilities allow charge-free imaging and analysis of non-conducting and hydrated samples. The Bruker spectrometer is paired with an X-Flash Silicon Drift Detector (SDD) with Hybrid Pulse Processing.

#### Micro-Raman spectrometry (Raman)

To further determine the physical composition of the deposits in the wood samples, the samples were analyzed by micro-Raman spectroscopy. Micro-Raman experiments were conducted with a RENISHAW inVia Laser micro confocal Raman spectrometer equipped with a research-grade Leica microscope with a spatial resolution of <0.5  $\mu\text{m}$ . The spot diameter under

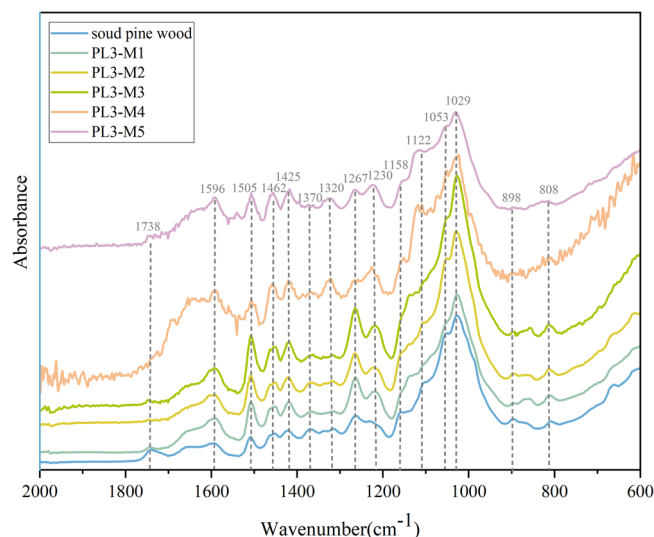


**Fig. 6** | FT-IR spectra for different wood samples.

the 50× objective was set at 3 $\mu$ m. The instrument uses a neon lamp as the signal source, 1800-line high-resolution grating, and UV and NIR simultaneously enhanced CCD detector—spectral range: 100 ~ 1600 nm. Excitation wavelength is 785 nm, laser power 280 mW, laser power density 0.5%, scanning time 10 s, scanning times 10 times. The spectrograms were analyzed using LabSpec5 software (Horiba, Kyoto, J). The spectra obtained were compared with a reference spectrum (RRUFF™ library).

## Results and discussion

### Assessment of the extent of wood degradation

Fourier Transform Infrared Spectrometer (FT-IR) is a commonly used instrumental analytical method for identifying archaeological wood's degradation degree. Wood mainly comprises three natural organic polymers: cellulose, hemicellulose, and lignin. The infrared-sensitive group of cellulose is hydroxyl, hemicellulose contains acetyl and hydroxyl groups, and lignin molecules contain methoxy, hydroxyl, carbonyl, carbon-carbon double bond, and benzene ring groups. Analyzing the presence or absence, position, shape, and intensity changes of these groups mentioned above through FT-IR makes it possible to evaluate the degree of degradation of different components by fingerprint data<sup>5,6</sup>. As wood degradation becomes more severe, the amount of hemicellulose in the wood gradually decreases, and the amount of lignin gradually increases. Therefore, the intensity ratio ( $I_{1505}/I_{1370}$ ) between the lignin absorption band (1505  $\text{cm}^{-1}$ ) and the hessian cellulose (1370  $\text{cm}^{-1}$ ) can be calculated to characterize the final degradation of wood in a semi-quantitative manner.

Three acquisitions were made for each sample using the infrared spectroscopy ATR mode and the peak area values of the samples at both 1505  $\text{cm}^{-1}$  and 1370  $\text{cm}^{-1}$  were obtained using the OMNIC™ software, and then the peak area values were used to calculate  $I_{1505}/I_{1370}$ . Cellulose has C-H bending vibrations at 896  $\text{cm}^{-1}$  of the infrared spectrum, cellulose and hemicellulose have C-H bending vibrations at 1367  $\text{cm}^{-1}$  wavelength, and lignin has C-O stretching at 1267  $\text{cm}^{-1}$  wavelength<sup>6</sup>. The results of infrared spectroscopy (Fig. 6) showed that the C-H absorption bands at 898  $\text{cm}^{-1}$  of cellulose in the wood samples PL3-M1, PL3-M2, and PL3-M3 were significantly weakened compared with those of sound pine wood, suggesting that cellulose in the wood of the ancient ship had been degraded to a certain extent. Meanwhile, the absorption bands at 898  $\text{cm}^{-1}$  for two samples, PL3-M4 and PL3-M5, hardly appeared, suggesting that cellulose in the untreated samples may be significantly degraded. The C-O stretching peak intensity at 1267  $\text{cm}^{-1}$  was significantly lower for untreated PL3-M4 and PL3-M5 samples, suggesting some lignin degradation in the unprotected treated wood. In addition, the C-H bending vibration peaks of cellulose and hemicellulose at 1367  $\text{cm}^{-1}$  almost disappeared in the untreated samples

**Table 1** | FTIR spectrometer detection results

Sample	Detection number	$I_{1505}/I_{1370}$	Average value
sound pine wood	1	1.63	1.70
	2	1.42	
	3	2.05	
PL3-M1	1	6.87	6.43
	2	5.94	
	3	6.47	
PL3-M2	1	7.17	7.96
	2	8.27	
	3	8.45	
PL3-M3	1	9.77	9.04
	2	9.27	
	3	8.07	
PL3-M4	1	12.93	13.87
	2	15.13	
	3	13.57	
PL3-M5	1	15.85	14.92
	2	13.67	
	3	15.24	

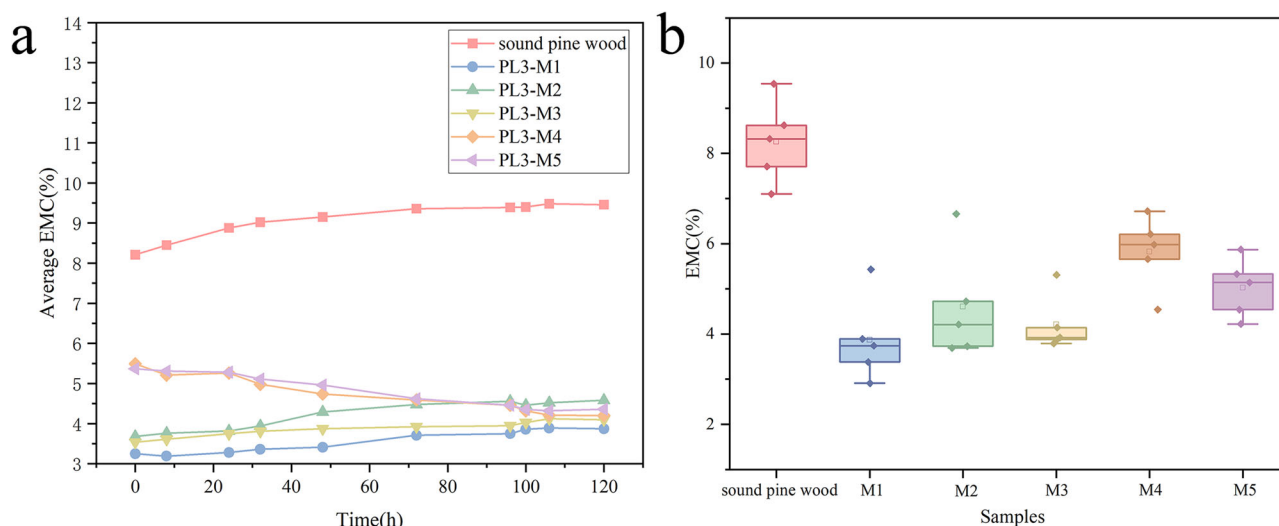
(PL3-M4 and PL3-M5), suggesting that cellulose and hemicellulose were highly degraded in unprotected treated wood compared to protected treated wood.

The results of  $I_{1505}/I_{1370}$  ratio calculations (Table 1) show that the  $I_{1505}/I_{1370}$  ratio of the Penglai III shipwreck samples is higher than that of the sound pine samples (the average  $I_{1505}/I_{1370}$  ratio value is 1.70). The mean  $I_{1505}/I_{1370}$  values for samples PL3-M1, PL3-M2, and PL3-M3 ranged between 6.43 and 9.04, while the mean  $I_{1505}/I_{1370}$  values for samples PL3-M4 and PL3-M5 were higher, at 13.87 and 14.92. The results indicate that the treated samples, although degraded to a certain extent, in contrast to the unprotected shipwreck wood, the degradation was more severe. This suggests that the previous protective treatments had a protective effect on the wood.

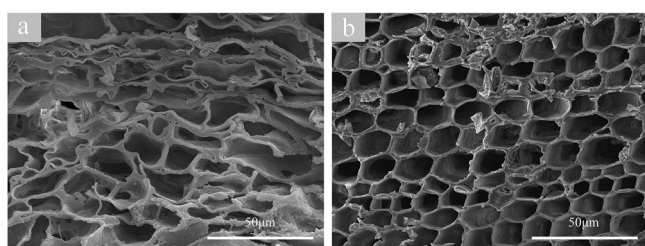
### Drying and consolidation status of wood

Figure 7 illustrates the results of equilibrium moisture content tests on samples of sound pine wood and wood from the wreck of Penglai III. For each sample, five different areas were selected for testing. As can be seen in Fig. 7-a, the moisture content of each sample stabilized at roughly day 5. The results (Fig. 7-b) show that the equilibrium moisture content of the sound pine wood is higher, ranging from 7.10 to 9.54%. Cells and wood tissues in sound wood are typically filled with water, both free water (e.g., in cell cavities) and water of crystallization. This water contributes to the high moisture content of sound wood. Different ancient samples had different values of moisture content, with a minimum value of 2.91% and a maximum value of 6.66% for treated samples. They are mainly distributed between 3.5% and 4.5%. The equilibrium water content of PL3-M4 and PL3-M5 is higher than that of the other ancient ship samples, mainly distributed between 4.5% and 6.0%. The moisture content of the wood samples has a certain impact on the long-term preservation of wood, and test results showed that the moisture content of the wood samples of the ancient ships tested is significantly low. This means that the ancient shipwreck of Penglai III has now been dehydrated and reached a more desirable dry state after PEG treatment. Removing the effect of specificity, the moisture content of the treated samples was lower than that of the untreated samples, probably due to the filling of PEG into the cellular structure of the samples.

The scanning electron microscope image (Fig. 8-b) of the cross-section of PL3-M2, a sample from the Penglai III shipwreck, showed that



**Fig. 7 | Test results of equilibrium moisture content of samples.** **a** Variation of the water content of different samples at 20 °C and 65% of temperature; **b** box plot of final equilibrium moisture content results for different samples.



**Fig. 8 | SEM image of the cross profile of samples.** **a** Sample PL3-M4; **b** sample PL3-M2.

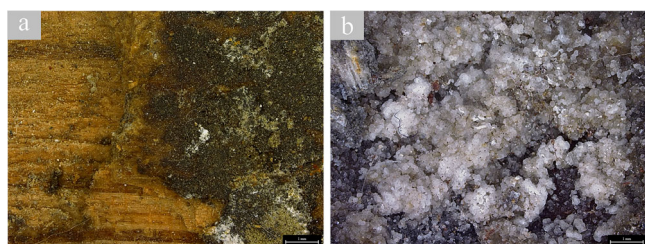


**Fig. 9 | Microscopic observation of sample PL3-M1.** **a** Black substance on the surface of sample PL3-M1 (50×); **b** White particles on the surface of sample PL3-M1 (30×).

the wood structure and cell lumen of the sample after drying and strengthening had a slight deformation and maintained the shape of the original waterlogged state. The image in Fig. 8-a shows that the wood cell structure of sample PL3-M4 was extruded and deformed severely, indicating that the PEG-treated sample underwent obvious deformation during the drying process. The appearance of the samples (Fig. 5) also shows that cracking and deformation occurred on the surface of both PL3-M4 and PL3-M5 wood. This comparison indicates that PEG materials play an important role in maintaining the structural stability of wood during the drying process.

As can be seen from Fig. 9, the surface of the sample was black as if covered with a black conjunctiva (Fig. 9a), with white crystalline particles distributed locally Fig. 9-b). The FTIR spectrometer analyzed the black substance and white particles on the surface of the wood, and the results are shown in Fig. 10. The infrared spectra of the black substance and the white

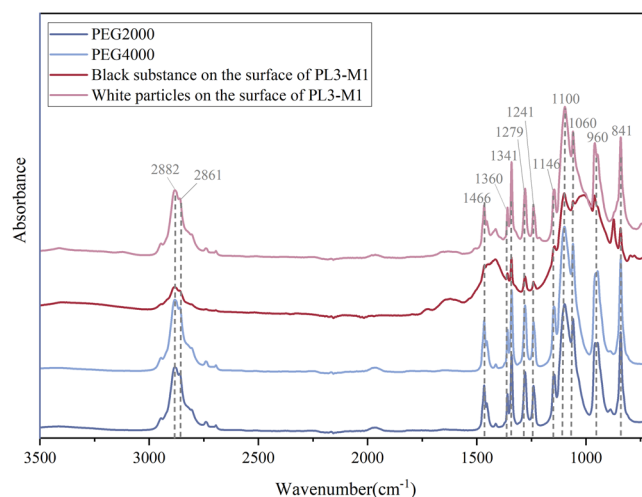


**Fig. 10 | FT-IR spectra of PEG2000, PEG4000, black material and white crystal on the surface of sample PL3-M1.**

particles showed a high degree of similarity, and the positions of their absorption bands were the same. It is well-established that the infrared absorption functional groups of PEG are mainly concentrated in the following: H-C-H symmetric stretching vibration attributed to the absorption bands at 2882  $\text{cm}^{-1}$  and 2861  $\text{cm}^{-1}$ ; H-C-H bending vibration attributed to the splitting bimodal bands at 1466  $\text{cm}^{-1}$  and 1455  $\text{cm}^{-1}$ ; absorption bands at 1360  $\text{cm}^{-1}$ , 1341  $\text{cm}^{-1}$ , 1279  $\text{cm}^{-1}$ , and 1241  $\text{cm}^{-1}$ . The absorption bands at 1360  $\text{cm}^{-1}$ , 1341  $\text{cm}^{-1}$ , 1279  $\text{cm}^{-1}$ , and 1241  $\text{cm}^{-1}$  are attributed to H-C-H out-of-plane oscillations; the absorption bands at 1146  $\text{cm}^{-1}$ , 1100  $\text{cm}^{-1}$ , and 1060  $\text{cm}^{-1}$  are attributed to C-O telescoping vibrations of the PEG molecule; and the absorption bands at 960  $\text{cm}^{-1}$ , 947  $\text{cm}^{-1}$ , and 841  $\text{cm}^{-1}$  are attributed to the in-plane oscillations of the H-C-H of the PEG molecule. The absorption bands of black substances and white crystals are mainly concentrated in the vicinity of 2882  $\text{cm}^{-1}$ , 2861  $\text{cm}^{-1}$ , 1466  $\text{cm}^{-1}$ , 1360  $\text{cm}^{-1}$ , 1341  $\text{cm}^{-1}$ , 1280  $\text{cm}^{-1}$ , 1240  $\text{cm}^{-1}$ , 1145  $\text{cm}^{-1}$ , 1100  $\text{cm}^{-1}$ , 1060  $\text{cm}^{-1}$ , 960  $\text{cm}^{-1}$ , 841  $\text{cm}^{-1}$ , which coincided with the positions of the peaks of PEG absorption. Therefore, the black conjunctiva and white particles on the surface of PL3-M1 should be PEG( $\text{HO}-(\text{C}_2\text{H}_4\text{O})_n\text{-H}$ ). The current darkening of the wood and localized precipitation of white crystals may have been caused by the spraying of PEG during the early conservation work on the ship.

PEG has been widely used as a common filler material for drying and strengthening ancient wooden shipwrecks<sup>8–11</sup>. First of all, it can be affirmed that PEG has many advantages in drying and reinforcing wood<sup>12</sup>. PEG can dehydrate and reinforce water-saturated wooden artifacts by penetrating the wood and replacing the water in water-saturated archaeological wood with water-soluble compounds that replace the water's supportive role<sup>13</sup>. For example, PEG4000 is more uniformly distributed at the cellular level of wood, and after reinforcement, wood porosity is reduced, cell longitudinal modulus of elasticity and hardness are increased, and dimensional stability is increased. Moreover, PEG materials are inexpensive and easily available. Therefore, PEG materials with different concentrations and molecular weights have been used for the dewatering and strengthening of water-saturated wood artifacts all over the world. For example, low molecular weight PEGs are highly hygroscopic and tend to cause swelling or even cracking of wood due to moisture absorption<sup>14–16</sup>. Under high temperatures and high humidity, PEG is easily lost and thus loses its reinforcing effect on the wood<sup>17,18</sup>. In addition, PEG is prone to redox reactions with metal ions and sulfates remaining in the wood, producing acidic substances, leading to further degradation of the wood and damaging its properties<sup>19</sup>.

In addition to these effects, PEG can cause changes in the appearance and color of waterlogged wood<sup>20</sup>, and Penglai III shipwreck is a good example of this problem. Different aspects of the causes of discoloration of PEG-treated wood have been studied and researched. Factors such as the structural characteristics of the wood, the degree of decay<sup>21</sup>, the iron content of the wood<sup>22</sup>, the chemical structure of the cell wall components and their content<sup>23</sup>, and whether or not to pass through the buffer solution treatment<sup>24</sup>, etc., may have an impact on the color change of the PEG treated wood. Since the spraying process was used instead of the soaking method for the Penglai III shipwreck during the early treatment, some of the PEG materials stayed on the surface of the samples for a long time, resulting in changes in the surface morphology and color of the wood. This effect on the appearance of wood will affect the exhibition effect to a certain extent and is not conducive to the long-term protection of wood. Therefore, in the conservation of marine wooden artifacts, it is very important to remove as many iron deposits as possible from the wood before the reinforcement treatment, as well as to reinforce the wood according to the state of preservation of different samples. At the same time, materials such as silicone compounds<sup>25,26</sup>, sugar alcohols<sup>27–30</sup>, vinyl materials<sup>31</sup>, cellulose, and its derivatives<sup>32,33</sup> and other materials can be considered to be selected for the reinforcing treatments, and the unfavorable impacts of the reinforcing materials on the wood can be avoided as much as possible. In addition, freeze-drying<sup>34</sup> and supercritical fluid drying<sup>35</sup> methods can be applied with some consideration depending on the situation. These two methods have been applied with good results in actual cases of shipwreck conservation. Choosing ways to desalinate and moisturize wood is also worthy of discussion and attention. From our experience, complete immersion of the boat timber in a soaking tank may give better results than the spraying method. Whether it is the removal of salt deposits in the wood or penetrating protective materials, the immersion method may be better. It is therefore considered that, where conditions are met, desalination and penetration of reinforcement should be carried out by immersion as far as possible, thus avoiding the undesirable effects of large quantities of impermeable chemical materials remaining on the surface of the wood.

### Deposited salts in the microstructure of wood

The pH values were examined for different parts of the wood sample surface of the Penglai III shipwreck (Fig. 11), and the results are shown in Table 2. The results showed that the pH of the rust-contaminated wood was all acidic, with the lowest pH value of 3.87, the highest of 4.65, the mean value of 4.26, and the median value of 4.21. The better-preserved parts of the wood had a neutral or alkaline pH, ranging from 6.74 to 8.55, and the mean value was 7.85. Pine pH generally ranged from 4 to 6 and was often related to the degree of decay. The pH of healthy pine wood has been tested at 6.24. The pH of individual rust-contaminated wood of the Penglai III shipwreck was lower than 4, and there was acidification. Iron deposits in the marine

environment react with oxygen in the water to form iron oxides. These iron oxides can release hydrogen ions (H<sup>+</sup>), making the surrounding environment acidic. When these iron deposits adhere to the surface of wooden artifacts, they gradually release hydrogen ions, leading to the acidification of the surface environment of the artifacts. At the same time, the rest of the well-preserved parts did not show any obvious acidification phenomenon. The wood was previously sprayed with a chemical such as borax, a 0.4% borax solution would typically have a pH between 9 and 10, which could be the cause of the localized alkalinity of the wood.

Acidification of wood out of the sea is often related to deposits<sup>36</sup>. Optical microscopy observations showed that many deposits were found on the surface of the samples. Traces of reddish-brown rust contamination were found on PL3-M1 (Fig. 12-a), PL3-M2 (Fig. 12-c), and PL3-M3 (Fig. 12-e), unevenly covering the sample surfaces. In addition, yellow, light yellow, and white deposits were found attached to the surface of all three wood samples (Fig. 12-b, Fig. 12-d, and Fig. 12-f). Red and yellow deposits were also found on the surface of both untreated PL3-M4 and PL3-M5 samples (Fig. 12-g and Fig. 12-h).

The SEM image of the cross profile of sample PL3-M2 (Fig. 13) showed that some of the wood cell cavities are filled with many deposits. The distribution of Fe elements and the morphology and distribution of deposits in the cell cavities of the wood are almost identical and more concentrated through the energy spectrum analysis. The elemental sulfur distribution overlaps the wood's cell walls and in some cell cavities. In addition, elemental calcium is also enriched and distributed to some extent, which is more in line with the range of distribution of the cellular structure. The above results show that Fe, S, and Ca are important elements in the deposits in the wood of Penglai III shipwreck, and there are some differences in the distribution of different elements.

ESEM-EDS also observed deposits of crystals of different morphologies in the cross-section of the samples. For example, tetragonal prismatic crystals were observed in Sample PL3-M1 (Fig. 14-a), and the spectral region showed that the atomic percentages of Fe and S are approximately 1:1 (Table 3), indicating that it is likely to be mackinawite (FeS). In addition, smooth rectangular lamellar crystals were observed in sample PL3-M1 (Fig. 14-b), with Ca and S as the main constituent elements, possibly CaSO<sub>4</sub>. In sample PL3-M2 (Fig. 14-c), a large number of strawberry-shaped spherical particles were observed filling the cellular cavities of the wood. The detection of the energy spectral region showed that the atomic ratio of Fe and S was about 1:2 (Table 3), probably pyrite framboids (FeS<sub>2</sub>). Needle-like crystal particles were observed in sample PL3-M3 (Fig. 14-d), and the sedimentary salt crystals were detected by the energy spectrum region to be high in iron and oxygen content (Table 3), which should be highly oxidized iron compounds. The presence of iron deposits was also found in sample PL3-M4 (Fig. 14-e,f), and energy spectroscopy results showed that the oxygen content of iron deposits was somewhat higher in PL3-M4 relative to treated wood (60.4% and 45.9%), suggesting that the degree of oxidation of iron deposits may have been higher in the untreated wood. The SEM results of sample PL3-M5 (Fig. 14-g) showed that the deposits in the wood contained a certain amount of calcium and sulfur, in addition to small amounts of silicon and magnesium. In addition, Fig. 14-h shows that there are a large number of spherical microorganisms distributed in the wood cell structure, closely attached to the wood cell wall, or filled in the wood tubular cell structure in an aggregated form. It indicates that the sample is seriously contaminated by microorganisms.

Microscopic Raman spectroscopy was utilized to determine further the physical composition of deposits in the wood samples from the Penglai III shipwreck. In PL3-M1, light yellow particles (Fig. 15) were detected as sulfur (S); reddish-brown deposits were goethite (FeOOH) (Fig. 16); and white particles were anhydrite (CaSO<sub>4</sub>) (Fig. 17). In addition, pyrite (FeS<sub>2</sub>) was detected in the PL3-M2 sample (Fig. 18). Hematite (Fe<sub>2</sub>O<sub>3</sub>) and aragonite (CaCO<sub>3</sub>) were also detected in the PL3-M3 sample (Figs. 19 and 20). The results of these tests indicated that the deposits in the wood samples consisted mainly of iron and calcium deposits, with the iron deposits including sulfur-iron compounds and oxidized state iron deposits.

**Fig. 11** | pH value testing area for samples PL3-M1, PL3-M2, and PL3-M3.

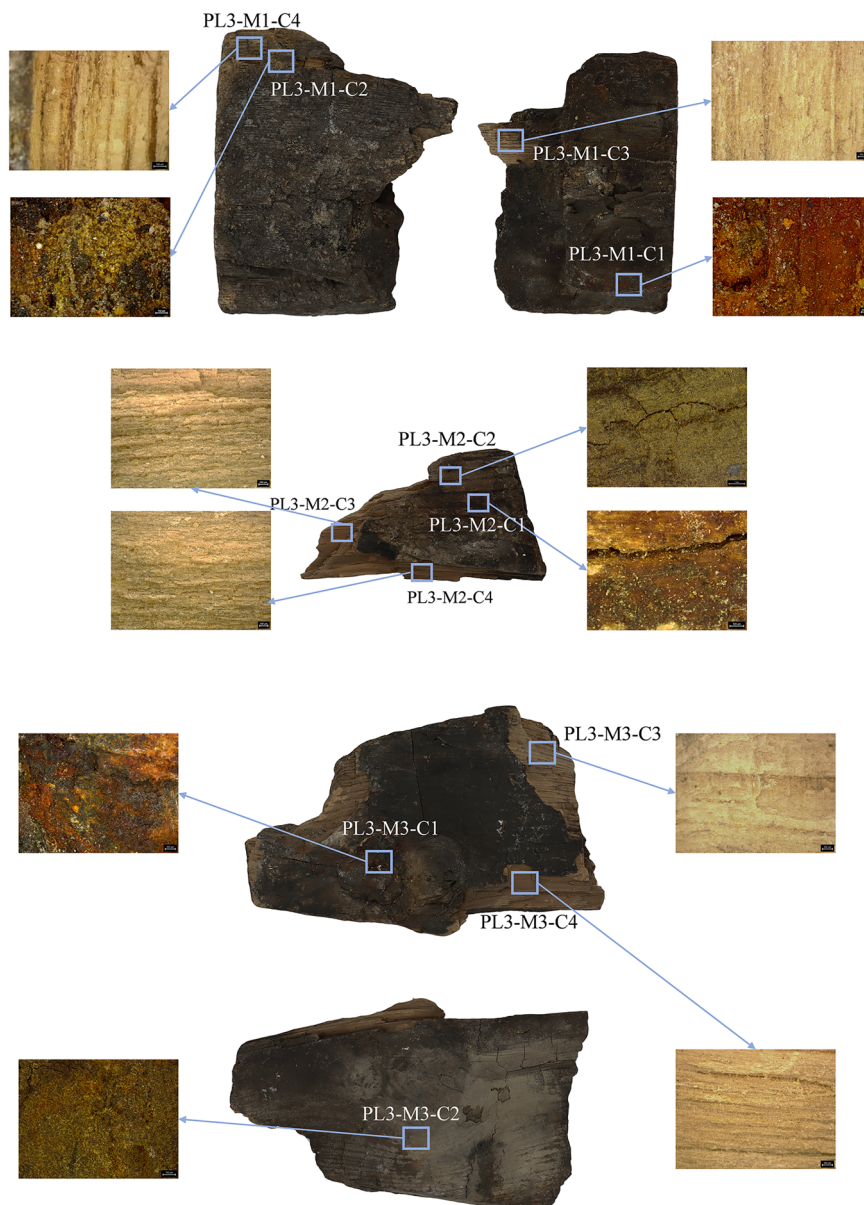


**Table 2** | Results of wood pH testing

Sample Number	Condition of the sampling site	pH
Sound pine wood	Uncontaminated	6.24
PL3-M1-C1	Contaminated with rust, reddish brown	4.65
PL3-M1-C2	Contaminated with rust, yellow-brown	4.56
PL3-M1-C3	Uncontaminated by rust	8.55
PL3-M1-C4	Uncontaminated by rust	8.37
PL3-M2-C1	Contaminated with rust, yellow-brown	4.10
PL3-M2-C2	Contaminated with rust, yellow-brown	3.87
PL3-M2-C3	Uncontaminated by rust	7.87
PL3-M2-C4	Uncontaminated by rust	7.36
PL3-M3-C1	Contaminated with rust, reddish brown	4.33
PL3-M3-C2	Contaminated with rust, yellow-brown	4.07
PL3-M3-C3	Uncontaminated by rust	6.74
PL3-M3-C4	Uncontaminated by rust	8.21

This result has similarities with the deposits on other marine shipwrecks. For example, the VASA began to show high acidity and rapid diffusion of sulfate on many of its plank surfaces starting in 2000<sup>37</sup>. These deposits were analyzed to be mainly  $KFe_3(SO_4)_2(OH)_6$ ,  $FeSO_4 \cdot 7H_2O$ ,  $S_8$ ,  $CaSO_4$ , and  $FeS_2$ <sup>38</sup>. The wood of the Mary Rose also contained sediments such as mercaptans (R-SH), disulfides (R-SS-R') and  $S_8$ ,  $FeS_2$ <sup>39</sup>. China's Nanhai I shipwreck was slightly later than the Penglai III shipwreck salvage (2007). Analyses in 2022 indicated that most of the iron deposits in the wood of this shipwreck were highly oxidized (e.g.,  $FeCO_3$ ,  $FeOOH$ , and  $Fe_3O_4$ ) and that much of the wood had become acidified and underwent significant degradation<sup>40</sup>. For wooden shipwrecks out of the sea, iron sulfide compounds and other deposits will cause harm and influence wood.  $FeS_2$  and other iron sulfide compounds easily oxidize and generate sulfuric acid in the presence of water and oxygen, causing further degradation of cellulose in the wood, which has already been damaged<sup>41</sup>. The redox reaction between  $Fe^{2+}/Fe^{3+}$  will play a catalytic role in oxidizing the iron sulfide compounds and degrading the organic matter<sup>19</sup>. Moreover, with the gradual oxidation of  $Fe^{2+}/Fe^{3+}$ , the unit molecular volume expands, and once water is lost and precipitated, it will cause stress damage to wood fibers<sup>42</sup>. Although many of the iron deposits in the Penglai III shipwreck are in a reduced state, the

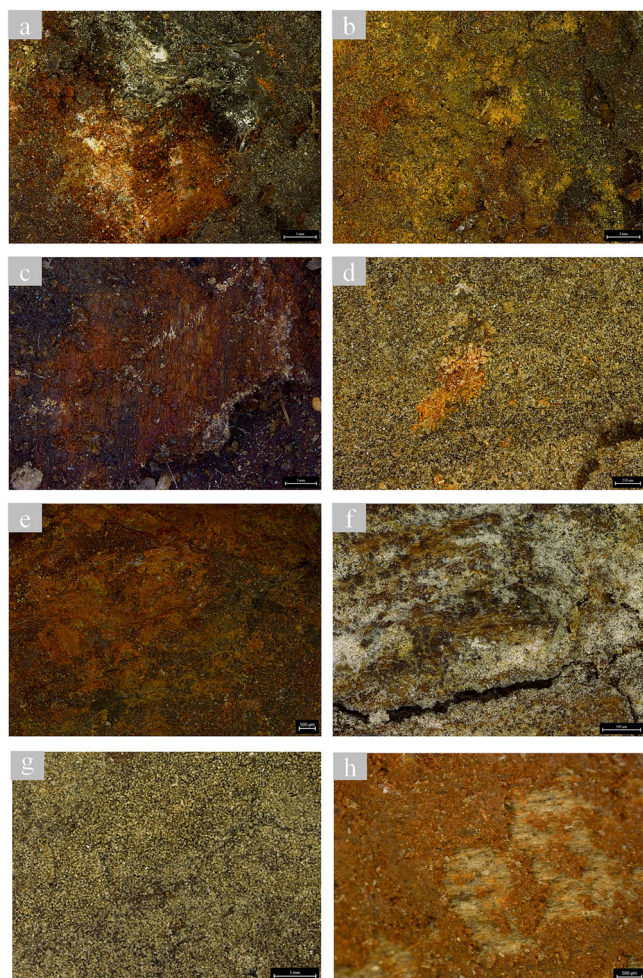


**Fig. 12 | Micro-morphological images of surface deposits on wood samples.** **a** Reddish brown deposits on the surface of PL3-M1; **b** Yellow deposits on the surface of PL3-M1; **c** Reddish brown deposits on the surface of PL3-M2; **d** Light yellow deposits on the surface of PL3-M2; **e** Reddish brown deposits on the surface of PL3-M3; **f** Light yellow and white deposits on the surface of PL3-M3; **g** Yellow deposits on the surface of PL3-M4; **h** Red deposits on the surface of PL3-M5.

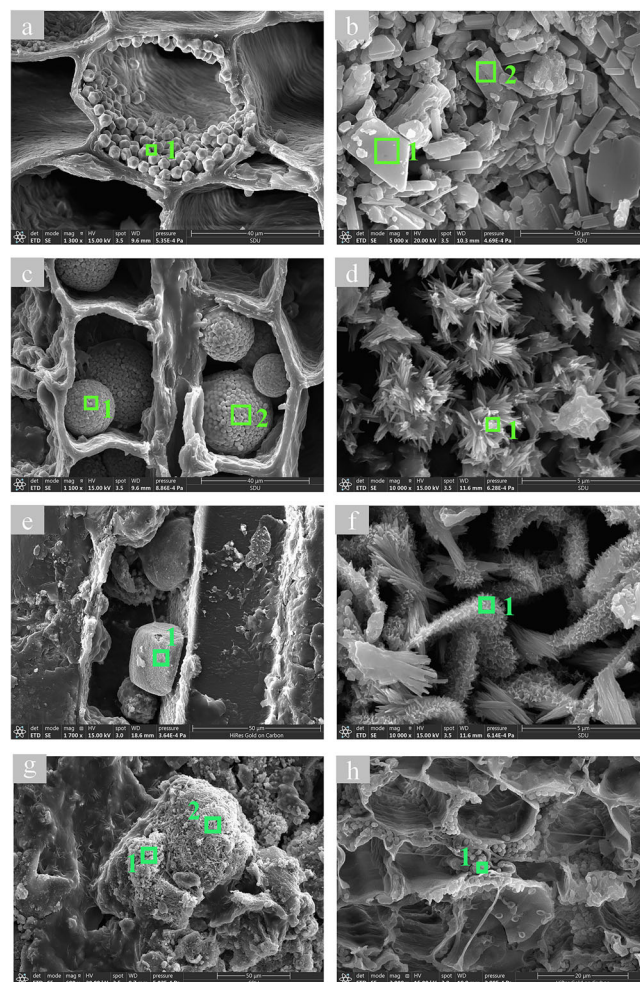


**Fig. 14 | SEM image of samples.** **a** Mackinawite crystals in sample PL3-M1; **b** Pyrite framboids crystals in sample PL3-M1; **c** Calcium sulfate crystals in sample PL3-M2; **d** Deposit crystals in sample PL3-M3; **e** Deposit crystals in sample PL3-M4; **f** Deposit crystals in sample PL3-M4; **g** Deposit crystals in sample PL3-M5; **h** Microorganisms in sample PL3-M5.

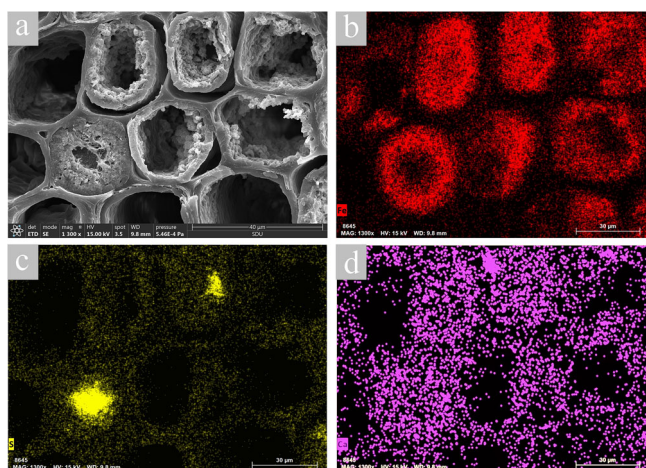


**Fig. 13 | Photomicrographs of wood section and element distribution of sample PL3-M2.** **a** SEM photographs; **b-d** surface scanning distribution photographs of different elements.

results show that some of them have been oxidized, which may pose potential hazards to the safety of the shipwreck.

In the early years of the shipwreck excavation, the shipwreck was large, and at that time, it did not have the conditions to build a large-scale immersion pool to remove the deposits. People could only use the spray or paste to continuously remove the deposits on the surface of the ship's wood, the effect was weak. At present, the ship's timbers are still heavily filled with deposits, and the timbers have been acidified locally, which is not conducive to the long-term preservation of the shipwreck. Therefore, subsequent consideration may be given to cleaning the surface of the ship's wood where deposit precipitation is more serious. However, the shipwreck has been dried to a dry state, and it is impossible to completely remove all the sediments in the shipwreck. Whether it is pyrite and other sulfur and iron compounds in the wood or iron sediments that have been oxidized, moisture is an important condition for their change and oxidation. So, the temperature and humidity control of the shipwreck's environment is particularly important. For example, the sulfate eruptions on the Batavia<sup>43</sup> and Vasa<sup>44</sup> wrecks were associated with environmental changes, especially changes in humidity. When the ambient humidity jumps above 70% RH, precipitation of sedimentary salts is likely to occur. At the same time, the ambient temperature where the two shipwrecks are located is generally maintained at about 20 °C. Wooden cultural relics' preservation of humidity requirements is more stringent; environmental humidity is too low, easily

**Table 3 | SEM-EDS results of deposits (at.%) in Fig. 14**

Analyzed point	C	O	Na	Si	Mg	S	Ca	Fe	N
Figs. 14a-1	16.9	6.5	0.4	—	—	37.2	1.9	37.1	—
Figs. 14b-1	18.0	34.4	—	—	—	23.8	24.9	—	—
Figs. 14b-2	6.8	26.2	—	—	—	31.6	30.9	—	—
Figs. 14c-1	49.8	10.6	0.3	—	—	25.5	—	13.8	—
Figs. 14c-2	52.8	6.5	—	—	—	27.2	—	13.5	—
Figs. 14d-1	31.8	43.8	—	—	—	—	—	24.4	—
Figs. 14e-1	25.2	60.4	—	—	—	0.65	—	13.8	—
Figs. 14f-1	27.8	45.9	—	—	—	—	—	26.3	—
Figs. 14g-1	10.9	55.3	—	5.0	—	11.9	16.2	0.8	—
Figs. 14g-2	6.4	72.4	8.7	1.2	0.9	—	10.1	—	—
Figs. 14h-1	57.8	28.2	—	—	—	—	0.4	—	13.6

“—” indicates that the elemental content is below the detection limit.

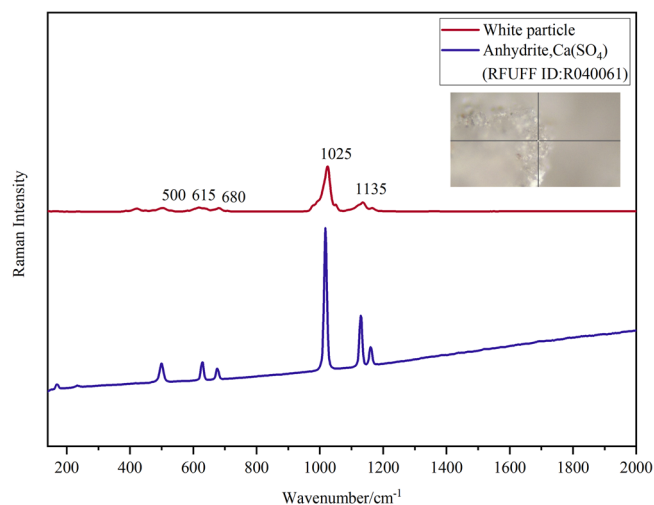


**Fig. 17 | Raman spectra of white particles on the surface of PL3-M1.**

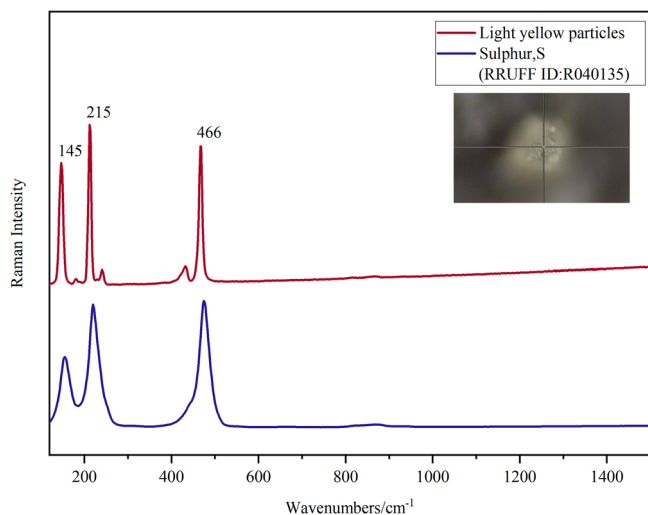


**Fig. 15 | Raman spectra of light yellow particles on the surface of PL3-M1.**

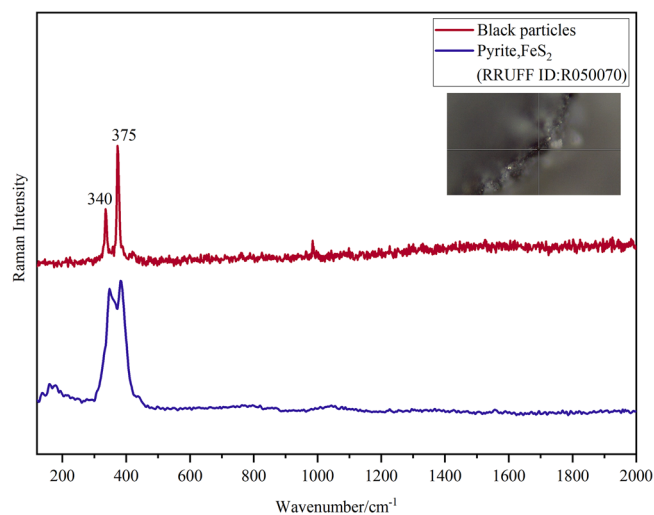


**Fig. 18 | Raman spectra of black particles on the surface of PL3-M2.**

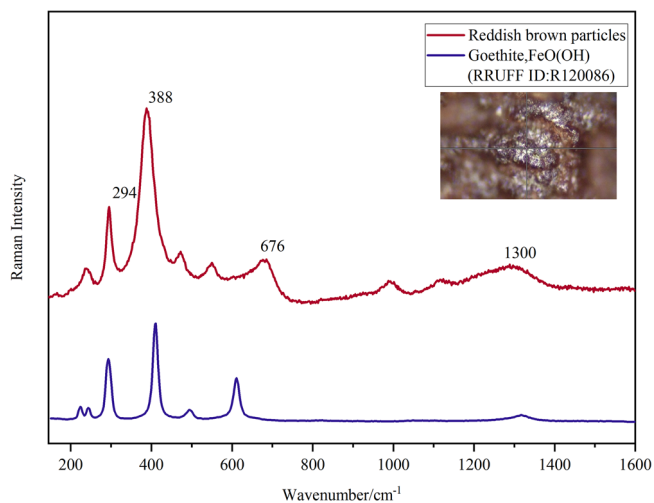


**Fig. 16 | Raman spectra of reddish brown particles on the surface of PL3-M1.**

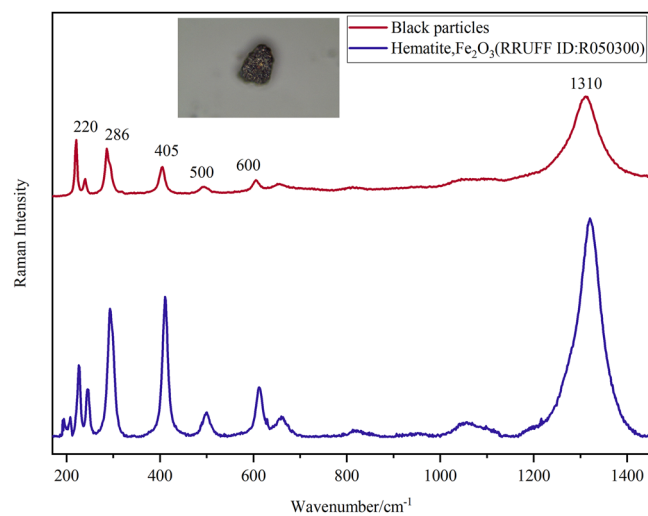


**Fig. 19 | Raman spectra of black particles on the surface of PL3-M3.**

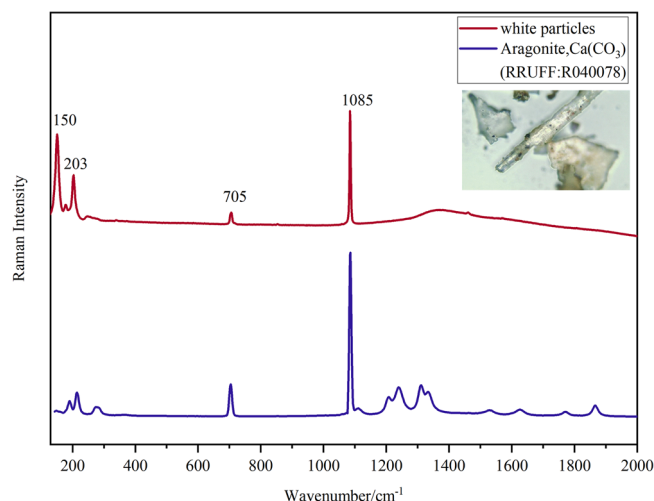


**Fig. 20** | Raman spectra of white particles on the surface of PL3-M3.

leads to wood cracking; humidity is too high and easily leads to sediment precipitation and microbial growth. Penglai Water City is located in the northern hemisphere in the mid-latitude region, is a warm temperate monsoon zone continental climate, with an average annual temperature of 12.5 °C, an average yearly maximum daily temperature of 28.8 °C, the average annual minimum daily temperature -2.3 °C, the extreme maximum temperature of 38.8 °C, the extreme minimum temperature -14.9 °C, the average yearly precipitation of 664 millimeters, the average annual relative humidity of 65%. Since the museum is near the sea, controlling relative humidity inside the museum is a difficult problem. During the summer rainy season, the relative humidity inside the museum is often higher than 70% RH, and the temperature and humidity difference between morning and evening is large. This situation is not conducive to the control of sedimentary salts. In the future, we should pay attention to the preventive conservation of shipwrecks and take corresponding measures to regulate the temperature, humidity, and light in the museum, preferably controlling the temperature at about 20 °C and the relative humidity at about 65%. Priority should be given to light sources in the gallery that do not produce ultraviolet rays or that can effectively reduce ultraviolet rays. A UV intensity meter can be installed to regularly check the level of UV light in the exhibition hall.

In conclusion, while the wooden artifacts from the Penglai III shipwreck have experienced some degradation, the  $I_{1505}/I_{1370}$  ratio of the treated wood is lower than that of untreated wood, indicating that the conservation treatment applied approximately 20 years ago has helped delay further deterioration. During the initial conservation phase, the hull was treated with polymer PEG, which successfully mitigated cracking and deformation, providing some reinforcement. The EMC of the treated samples ranged from 2.91% to 6.66%, which has reached a more desirable dry state. However, PEG accumulation on the surface caused the darkening of the wood, negatively impacting the wreck's appearance. This highlights the potential drawbacks of PEG in wood preservation.

Additionally, deposits of iron (e.g., sulfur-iron compounds) and calcium deposits have accumulated both on the surface and within the wood's cellular structure. Over time, these deposits can cause acidification and accelerate decay, complicating long-term preservation efforts. As desalination of dry wood is challenging, future conservation efforts should focus on stricter control of temperature and humidity to better preserve the wood. Only by continuously assessing the conservation status of cultural relics from the perspective of sustainable development and actively solving emerging problems can the long-term protection of these precious relics be truly strengthened.

### Data availability

No datasets were generated or analysed during the current study.

Received: 14 October 2024; Accepted: 23 April 2025;

Published online: 20 May 2025

### References

- Shandong Institute of Cultural Heritage and Archaeology Yantai Museum, Penglai Cultural Relics Bureau. Ancient ship of Penglai. Beijing: *Cultural Relics Press*. 3-17+73-78 (2006). (in Chinese).
- Yuan, X. C. Briefing on the Excavation of Three Ancient Ships in Penglai. *Res. History Maritime Transp.* 1-19 + 135-136 (2006). (in Chinese).
- Yuan, X. C. Exploration of Protection Technology in the Protection Process of Three Ancient Ships in Penglai. *Proceedings of the Sixth Academic Annual Conference of China Association for the Protection of Cultural Relics Technology*. **5**(2009). (in Chinese).
- China - National Standard (CN-GB). Determination of wood pH (GB/T 6043-2009), Beijing, National Technical Committee for Wood Standardization. (2009). (in Chinese).
- Fors, Y., Jalilehvand, F. & Sandström, M. Analytical Aspects of Waterlogged Wood in Historical Shipwrecks. *Anal. Sci.* **27**, 785–792 (2011).
- Almkvist, G., Norbakhsh, S., Bjurhager, I. & Varmuza, K. Prediction of tensile strength in iron-contaminated archaeological wood by FT-IR spectroscopy – a study of degradation in recent oak and Vasa oak. *Holzforschung*. **70**, 855–865 (2016).
- Irina et al. New versatile approach for analysis of PEG content in conjugates and complexes with biomacromolecules based on FTIR spectroscopy. *Colloid Surf. B*. **141**, 36–43 (2016).
- Glastrup, J. Degradation of polyethylene glycol. A study of the reaction mechanism in a model molecule: Tetraethylene glycol. *Polym. Degrad. Stabil.* **52**, 217–222 (1996).
- Feng, N., Tzeng, Y. & Zhou, L. Conservation of waterlogged archaeological wood: what we can learn from the Vasa experience?. *Asian Archaeol.* **8**, 143–151 (2024).
- Majka, Z., Fejfer, W. & Herit, O. Dimensional stability and hygroscopic properties of PEG treated irregularly degraded waterlogged Scots pine wood. *J. Cult. Herit.* **31**, 133–140 (2018).
- Wang, X., Zhang, B., Hu, Y. & Zhu, L. Temporary solidifying extraction and in-situ preservation of fragile marine wooden artifacts: Experimental study and pilot test. *J. Cult. Herit.* **53**, 220–225 (2022).
- Han, L. Y. et al. Effects of three kinds of consolidants on the micromechanical properties of archaeological wood from “xiaobaijiao I” shipwreck by infrared spectroscopy and thermogravimetric analysis. *Spectrosc. Spectr. Anal.* **42**, 5 (2022). (in Chinese).
- Kawai, F. Microbial degradation of polyethers. *Appl Microbiol Biot.* **58**, 30 (2002).
- Walsh-Korb, Z. & Avérous, L. Recent developments in the conservation of materials properties of historical wood. *Prog. Mater. Sci.* **102**, 167–221 (2018).
- Xu, Q. M. et al. Progress of research on stereotypical reinforcement protection of water-saturated wooden cultural relics. *J. Shanghai Univ. (Nat. Sci. Ed.)*. **30**, 1006–1017 (2024). (in Chinese).
- Kl, A. G., Kl, N. & Arnold, D. C. Analyses of Sulfur and Iron in Waterlogged Archaeological Wood: The Case of Polyethylene-Glycol-Treated Yenikap 12 Shipwreck. *Forests*. **14**, 530 (2023).
- Broda, M. & Mazela, B. O. Application of methyltrimethoxysilane to increase dimensional stability of waterlogged wood. *J. Cult. Herit.* **25**, 149–156 (2017).
- Zhou, Y., Wang, K. & Hu, D. High retreatability and dimensional stability of polymer grafted waterlogged archaeological wood achieved by ARGET ATRP. *Sci. Rep.-Uk.* **9**, 9879 (2019).
- Almkvist, G. & Persson, I. Fenton-induced degradation of polyethylene glycol and oak holocellulose. A model experiment in comparison to changes observed in conserved waterlogged wood. *Holzforschung* **62**, 704–708 (2008).

20. Hoffmann, P. J. I. To be and to continue being a cog: the conservation of the Bremen Cog of 1380. *Int. J. Naut. Archaeol.* **30**, 129–140 (2001).
21. Han, L. Y. et al. The degree of constructional decay of water-saturated Qing dynasty wood and the effect of reinforcement treatment on its color. *J. Southwest Forestry Univ. (Nat. Sci.)*, **40**, 132–138 (2020). (in Chinese).
22. Zhao, G. F. et al. Exploring the reasons for the color change of ancient wet wood treated with polyethylene glycol in saturated water. *Cultural Relics Sci. Technol. Res.* **2**, 127–130 (2004). (in Chinese).
23. Gonzalez-Pena, M. M. & Hale, M. D. C. Colour in thermally modified wood of beech, Norway spruce and Scots pine. Part 2: Property predictions from colour changes. *Holzforschung* **63**, 394–401 (2009).
24. Qin, L. et al. Exploration of the causes of discoloration of wood remains by PEG reinforcement treatment. *J. Southwest Forestry Univ.* **38**, 173–179 (2018). (in Chinese).
25. Broda, M. & Plaza, N. Z. Durability of model degraded wood treated with organosilicon compounds against fungal decay. *Int. Biodeter. Biodegr.* **178**, 8 (2023).
26. Broda, M. & Yelle, D. J. Reactivity of Waterlogged Archeological Elm Wood with Organosilicon Compounds Applied as Wood Consolidants: 2D1 H-13 C Solution-State NMR Studies. *Molecules*. **11**, 3407 (2002).
27. Han, L. et al. Evaluation of PEG and sugars consolidated fragile waterlogged archaeological wood using nanoindentation and ATR-FTIR imaging. *Int. Biodeter. Biodegr.* **170**, 105390 (2022).
28. Rocha, M. B., Peyron, A. S., Lara-García, H. A., Felipe, C. & Lima, E. Preservation of wooden objects recovered from the recent archaeological excavations of the Great Temple in Tenochtitlan. *J. Cult. Herit.* **44**, 47–52 (2020).
29. Antonelli, F., Bartolini, M., Plissonnier, M. L., Esposito, A. & Romagnoli, M. Microorganisms Essential Oils as Alternative Biocides for the Preservation of Waterlogged Archaeological Wood. *Microorganisms*. **8**, 2015 (2020).
30. Liu, L., Zhang, L., Zhang, B. & Hu, Y. A comparative study of reinforcement materials for waterlogged wood relics in laboratory. *J. Cult. Herit.* **36**, 94–102 (2019).
31. Zhou, Y., Wang, K. & Hu, D. An aqueous approach to functionalize waterlogged archaeological wood followed by improved surface-initiated ARGET ATRP for maintaining dimensional stability. *Cellulose*. **28**, 2433–2443 (2021).
32. Fulcher, K. An investigation of the use of cellulose-based materials to gap-fill wooden objects. *Stud. Conserv.* **62**, 210–222 (2017).
33. Wakefield, et al. Aminoethyl substitution enhances the self-assembly properties of an aminocellulose as a potential archaeological wood consolidant. *Eur. Biophys. J. Biophys.* **49**, 791–798 (2020).
34. Broda, M., Curling, S. F. & Frankowski, M. The effect of the drying method on the cell wall structure and sorption properties of waterlogged archaeological wood. *Wood Sci. Technol.* **55**, 971–989 (2021).
35. Zhang, J., Yang, L. & Liu, H. Green and efficient processing of wood with supercritical CO<sub>2</sub>: A review. *Appl. Sci. (Switz.)*. **11**, 3929 (2021).
36. Zhang, H., Shen, D., Zhang, Z., Kang, H. & Ma, Q. Comparison of iron deposits removing material from the marine archaeological wood of Nanhai I shipwreck. *J. Cult. Herit.* **66**, 59–67 (2024).
37. Sandström, M., Jalilvand, F., Persson, I., Gelius, U. & Frank, P. Acidity and salt precipitation on the Vasa: the sulphur problem. In *Proc. 8th ICOM Group on Wet Organic Archaeological Materials Conference*: Stockholm, **2001**, 67–89 (2002).
38. Sandström, M., Jalilvand, F., Persson, I., Gelius, U. & Hall-Roth, I. Deterioration of the seventeenth-century warship Vasa by internal formation of sulphuric acid. *Nature* **415**, 893–897 (2002).
39. K., M. W., R., M. M., A., M. J. & A., D. Sulfur and iron speciation in recently recovered timbers of the Mary Rose revealed via X-ray absorption spectroscopy. *J. Archaeol. Sci.* **35**, 1317–1328 (2008).
40. Zhang, H., Shen, D., Zhang, Z. & Ma, Q. Characterization of degradation and iron deposits of the wood of Nanhai I shipwreck. *Herit. Sci.* **10**, 1–13 (2022).
41. Lindfors, E. L., Lindstroem, M. & Iversen, T. Polysaccharide degradation in waterlogged oak wood from the ancient warship Vasa. *Holzforschung* **62**, 57–63 (2008).
42. Fors, Y. Sulfur Speciation and Distribution in the Vasa's Wood Protection by water pollution leaves a sour aftertaste. 57–58 (2005).
43. Richards & Lewana, V. The consolidation of degraded deacidified batavia timbers. *Aiccm Bulletin*. **16**, 35–52 (1990).
44. Hocker, E. Maintaining a Stable Environment: Vasa's New Climate-Control System. *Bull. Assoc. Preserv. Technol.* **41**, 2–3 (2010).

## Acknowledgements

We thank the Institute of Humanities and Social Sciences [SK220693] and Shandong Provincial Science and Technology Department [2020YFC1521800b] for the financial support of this research under two fundings. The authors express their gratitude to Haojing Ning of Shandong University, Xiaochun Yuan, Meng Yang, Huiquan Fan, and Yuqian Wang of Penglai Pavilion Scenic Area for their kind support and assistance. Wood samples were supplied by the Penglai Ancient Ship Museum.

## Author contributions

Q.M. provided support and guidance for this study. Y.W. performed experiment analysis and drafted the manuscript. L.L. gave a great help in the preliminary research and sample collection. S.W. contributed to the discussion portion of this study. Z.L. assisted in this study. All authors read and approved the final manuscript.

## Competing interests

Q.M. is an Editorial Board Member of npj Heritage Science. However, he was not involved in the peer review process or decision-making for this manuscript. No other authors have conflicts of interest to disclose.

## Additional information

**Correspondence** and requests for materials should be addressed to Qinglin Ma.

**Reprints and permissions information** is available at <http://www.nature.com/reprints>

**Publisher's note** Springer Nature remains neutral with regard to jurisdictional claims in published maps and institutional affiliations.

**Open Access** This article is licensed under a Creative Commons Attribution-NonCommercial-NoDerivatives 4.0 International License, which permits any non-commercial use, sharing, distribution and reproduction in any medium or format, as long as you give appropriate credit to the original author(s) and the source, provide a link to the Creative Commons licence, and indicate if you modified the licensed material. You do not have permission under this licence to share adapted material derived from this article or parts of it. The images or other third party material in this article are included in the article's Creative Commons licence, unless indicated otherwise in a credit line to the material. If material is not included in the article's Creative Commons licence and your intended use is not permitted by statutory regulation or exceeds the permitted use, you will need to obtain permission directly from the copyright holder. To view a copy of this licence, visit <http://creativecommons.org/licenses/by-nc-nd/4.0/>.

© The Author(s) 2025